ELSEVIER

Journal of Molecular Catalysis A: Chemical 135 (1998) 199–208

JOURNAL OF MOLECULAR CATALYSIS A: CHEMICAL

Effects of non-stoichiometry of calcium and strontium hydroxyapatites on the oxidation of ethane in the presence of tetrachloromethane

Shigeru Sugiyama [a,*], Takashi Miyamoto [a], Hiromu Hayashi [a], John B. Moffat [b]

[a] *Department of Chemical Science and Technology, Faculty of Engineering, The University of Tokushima, Minamijosanjima, Tokushima 770-8506, Japan*

[b] *Department of Chemistry and the Guelph–Waterloo Centre for Graduate Work in Chemistry, University of Waterloo, Waterloo, Ontario, Canada N2L 3G1*

Received 28 August 1997; accepted 4 December 1997

Abstract

The effects of the introduction of tetrachloromethane (TCM) into the feedstream for the oxidative dehydrogenation of ethane have been investigated on stoichiometric and non-stoichiometric calcium and strontium hydroxyapatites (CaHAp and SrHAp, respectively) at 773 K. The conversion and selectivities in the presence of TCM were found to depend on the reaction conditions, as well as the stoichiometry and structural instability of the catalysts.

Keywords: Ethane; Oxidation; Hydroxyapatites; Chlorapatite; Non-stoichiometry; Tetrachloromethane

1. Introduction

The transformation of light alkanes such as methane and ethane into more valuable organic compounds is of considerable current interest. Although dehydrogenation is the simplest of processes, oxidative dehydrogenation has advantages thermodynamically [1]. However, almost inevitably, the oxidative dehydrogenation of alkanes produces carbon oxides because of the low selectivity of the catalyst employed. Among carbon oxides, carbon monoxide is a valuable feed stock as syngas for the production of basic chemicals such as 1,2-ethanediol [2–5], ethanol [6–8], acetic acid [9] and lower olefins [10]. The development of catalysts capable of activating the C–H bonds of the alkane molecule and suppressing the deep oxidation to CO_2 is of prime importance.

The oxidative dehydrogenation and partial oxidation of methane on various hydroxyapatites have been recently investigated in our laboratories. Calcium hydroxyapatites (CaHAp) can function as acidic and/or basic catalysts, depending on their composition [$Ca_{10-x}(HPO_4)_x(PO_4)_{6-x}(OH)_{2-x}$, $0 \le x \le 1$] [11–16], with sto-

* Corresponding author. Tel.: +81-886-567432; fax: +81-886-557025; e-mail; sugiyama@chem.tokushima-u.ac.jp

1381-1169/98/$ - see front matter
PII: S1381-1169(97)00305-1

ichiometric forms [17] in which $x = 0$ (Ca/P = 1.67, atomic ratio) containing acidic and basic sites, while non-stoichiometric versions [17] with $0 < x \leq 1$ ($1.50 \leq$ Ca/P < 1.67) are effective in acid-catalyzed processes [12]. However, X-ray diffraction (XRD) patterns of CaHAp are found to be essentially identical, regardless of the stoichiometry. In the oxidation of methane on stoichiometric and non-stoichiometric CaHAp, methane is predominantly converted to carbon oxides [18,19] while, on addition of tetrachloromethane (TCM) to the methane oxidation feedstream, the selectivity to carbon monoxide increased concomitant with the decrease of that to carbon dioxide and of the conversion of methane with increasing time-on-stream [20–22]. Similarly, strontium hydroxyapatites (SrHAp) consisting of various Sr/P ratios afford carbon oxides [23] while selectivities to carbon monoxide up to 80% are also observed in the absence of TCM [24,25]. Introduction of TCM resulted in further enhancement of the selectivity to carbon monoxide with an accompanying decrease in the conversion of methane, particularly with increasing time-on-stream [24,25]. Furthermore, the conversion and selectivity on CaHAp and SrHAp were influenced by the atomic ratios of Ca/P and Sr/P, respectively, regardless of the addition of TCM into the feedstream [21,24,25]. The previous results with hydroxyapatites demonstrate that the introduction of TCM into the methane oxidation feedstream has the principal effect of depressing deep oxidation processes, so that the formation of carbon dioxide is suppressed in favour of carbon monoxide, in contrast with the observations with other solid catalysts on which the selectivity to C_2 compounds, particularly ethylene, increases on addition of TCM [26].

Although considerable work has been reported on the introduction of TCM in methane oxidation, relatively little information is available on the effects of the chloromethane on oxidation processes with other light alkanes. In the present study, the effects of the introduction of a small amount of TCM into the feedstream for the oxidation of ethane at 773 K have been investigated on CaHAp and SrHAp consisting of various Ca/P and Sr/P ratios, respectively. In view of the earlier reports on the oxidation of methane on CaHAp [20–22] and SrHAp [24,25] in the presence of TCM, the effects of the concentration of TCM and oxygen on the ethane oxidation are examined and the catalysts previously employed in the oxidation in the presence of TCM are analyzed by both bulk and surface techniques.

2. Experimental

Calcium or strontium hydroxyapatites were prepared from $Ca(NO_3)_2 \cdot 4H_2O$ (Wako Pure Chemicals, Osaka) or $Sr(NO_3)_2$ (Wako), respectively, and $(NH_4)_2HPO_4$ (Wako) [19,23]. The resulting solid was calcined at 773 K for 3 h after drying in air at 373 K overnight. The sample after calcination is referred to as the 'fresh catalyst'. All catalysts were sieved to particle size of 1.70–0.85 mm. The concentrations of Ca, Sr and P in each catalyst were measured in aqueous HNO_3 solution with inductively coupled plasma (ICP) spectrometry. The catalysts are denoted as $CaHAp_{x.xx}$ or $SrHAp_{x.xx}$ with $x.xx$ equal to the atomic ratio of Ca/P or Sr/P in each catalyst as determined with ICP. The BET surface areas, apparent densities and the atomic ratios of Ca/P and Sr/P are summarized in Table 1.

The catalytic experiments were performed in a fixed-bed continuous-flow quartz reactor operated at atmospheric pressure. Details of the reactor design and operating procedure have been described elsewhere [20]. Prior to reaction, CaHAp [20–22] and SrHAp [24,25] were calcined in situ in an oxygen flow (12.5 ml/min) for 1 h at 973 and 873 K, respectively. Except as noted, reaction conditions were: $W = 0.5$ g, $F = 15$ ml/min, $T = 773$ K, $P(C_2H_6) = 27.1$ kPa, $P(O_2) = 6.7$ kPa and $P(TCM) = 0$ or 0.17 kPa; balance to atmospheric pressure was provided by helium.

The reactant and products were analyzed with an on-stream gas-chromatograph (Shimadzu GC-8APT) equipped with a TC detector and integrator (Shimadzu C-R6A). The column systems used in the present study and the procedures employed in the calculation of conversions and selectivities have been described previously [21,27].

Powder X-ray diffraction (XRD) patterns were recorded with a Rigaku RINT 2500X diffractometer, using monochromatized Cu–Kα radiation. Patterns were recorded over the 2θ range from 5°–60°. The XRD patterns of fresh CaHAp and SrHAp were essentially identical regardless of their Ca/P and Sr/P ratios and in agreement with the reference patterns $Ca_{10}(PO_4)_6(OH)_2$ [JCPDS 9-0432] and $Sr_{10}(PO_4)_6(OH)_2$ [JCPDS 33-13248], respectively. X-ray photoelectron spectrometry (XPS; Shimadzu ESCA-1000AX) used monochromatized Mg–Kα radiation. The binding energies were corrected using 285 eV for C 1s as an internal standard. Argon-ion etching of the catalyst was carried out at 2 kV for 1 min with a sputtering rate estimated as ca. 2 nm/min for SiO_2. The surface properties of fresh CaHAp and SrHAp determined with XPS are also summarized in Table 1.

3. Results and discussion

To minimize the contribution of the homogeneous oxidation of ethane, 773 K was selected as the reaction temperature for this work [27]. Under these conditions, the conversions of ethane and the selectivities on CaHAp showed little variation with the Ca/P ratios (Fig. 1A). With TCM in the feedstream, the conversion of C_2H_6 and the selectivity to CO_2 decreased while that to C_2H_4 increased with increasing time-on-stream on all stoichiometries of CaHAp. The enhancement of the selectivity to C_2H_4 was particularly evident on $CaHAp_{1.51}$ and $CaHAp_{1.60}$, on which the selectivity to CO remained unchanged with increasing time-on-stream (Fig. 1B). The XRD patterns of the catalysts after use in the oxidation process with TCM (Fig. 2) were significantly different from those of the fresh catalysts, showing the presence of calcium chlorapatite [$Ca_{10}(PO_4)_6Cl_2$: JCPDS 33-0271] and/or calcium phosphate [$Ca_3(PO_4)_2$: JCPDS 9-0169]. The XRD patterns of $CaHAp_{1.55}$ and $CaHAp_{1.64}$ showed that the bulk structure of these catalysts was converted from CaHAp into the corresponding phosphate and chlorapatite, respectively, during the oxidation with TCM. Since the catalytic activities on

Table 1
Bulk and surface properties of CaHAp and SrHAp

Catalyst	M/P[a]	S.A.[b]	B.D.[c]	Binding energy/eV			Atomic ratio[e]	
				O 1s	Ca 2p1/2 or Sr 3p1/2	P[d]	M/P[f]	O/M[f]
CaHAp	1.64	95.9	0.50	531.5	350.9	133.3	1.21	2.50
CaHAp	1.60	87.2	0.55	531.3	350.9	133.1	1.28	2.49
CaHAp	1.55	82.8	0.36	531.3	350.8	133.0	1.17	2.78
CaHAp	1.51	76.8	0.50	531.3	350.9	133.9	1.24	2.52
SrHAp	1.73	65.5	0.43	530.9	279.0	190.3	1.61	2.30
SrHAp	1.70	67.9	0.40	531.1	279.3	190.6	1.67	2.02
SrHAp	1.67	60.3	0.45	530.9	279.2	190.3	1.53	1.70
SrHAp	1.61	72.4	0.42	531.4	279.5	190.8	1.67	1.88

[a]Atomic ratio determined with ICP. M = Ca or Sr.
[b]Surface area (m^2/g).
[c]Bulk density (g/cm^3).
[d]P 2p for Ca and P 2s for Sr.
[e]As determined from XPS.
[f]M = Ca or Sr.

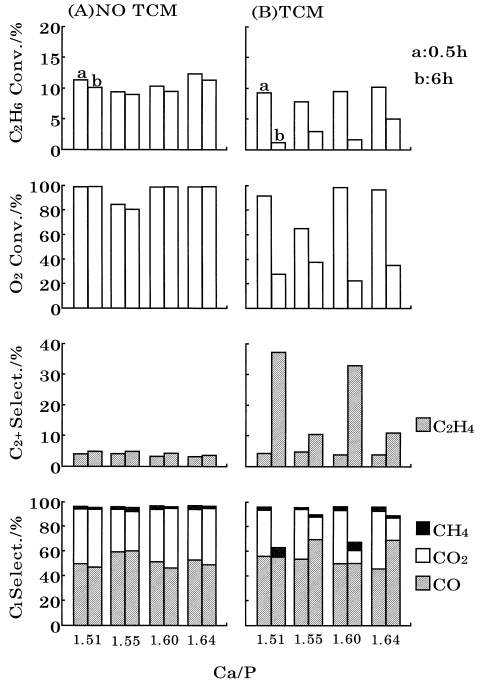

Fig. 1. Ethane oxidation on CaHAp in the absence (A) and presence (B) of TCM at 773 K. Conditions: $W = 0.5$ g, $F = 15$ ml/min, $P(C_2H_6) = 27.1$ kPa, $P(O_2) = 6.7$ kPa and $P(TCM) = 0.17$ kPa (when present) diluted with He.

both catalysts were essentially identical, their surface properties apparently exert a predominant influence in the oxidation in the presence of TCM. The surface regions of the samples previously employed in the oxidation of ethane with TCM were identical with those of the corresponding fresh catalysts from XPS analyses (Table 1) except for the existence of a peak due to Cl 2p at approximately 199 eV with all samples. However, the atomic ratio of Cl/Ca on each catalyst was strongly influenced by the atomic Ca/P ratio (Table 2). The Cl/Ca ratios of the used catalysts with Ca/P = 1.64 and 1.60 were not dependent on the argon-ion etching (Table 2) and their XRD patterns matched that of chlorapatite (Fig. 2), suggesting that the chlorinated species detected by XPS is calcium chlorapatite. In contrast, the Cl/Ca ratio on the surface of $CaHAp_{1.55}$ was larger than that after the etching (Table 2) and the XRD patterns indicated a mixture of the chlorapatite and calcium phosphate. Although the XRD patterns of used $CaHAp_{1.55}$ showed only one phase of the phosphate XPS analysis detected a chlorinated species in the near-surface regions (Table 2). It is difficult to identify the chlorinated species on the used $CaHAp_{1.55}$ but the formation of the corresponding chlorapatite or chloride is probable. Chlorapatite was also detected on commercial $Ca_3(PO_4)_2$ previously employed in the oxidation of methane with TCM [22]. The formation of this chloride appeared to have occurred on alkaline earth phosphates previously used in the oxidation of methane and ethane [26,27]. No direct correlation of the effect of the introduction of TCM on ethane oxidation with the amount of the chlorinated species in the near-surface region is evident (Fig. 1). These results undoubtedly show that, regardless of the introduction of TCM, the activities, the conversion from CaHAp to the corresponding chlorapatite or phosphate and the formation of the chlorinated species during the oxidation process are strongly influenced by the stoichiometry of CaHAp.

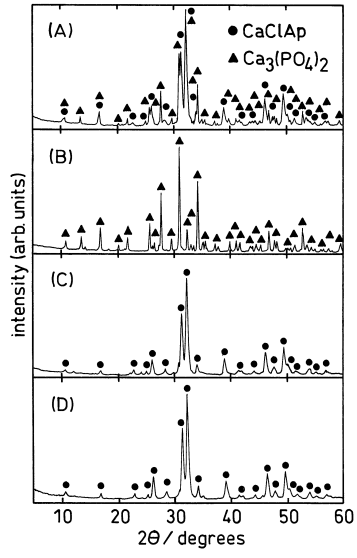

Fig. 2. XRD patterns of CaHAp previously employed in obtaining the results shown in Fig. 1B but after 6 h on-stream. (A) Ca/P = 1.51, (B) Ca/P = 1.55, (C) Ca/P = 1.60, (D) Ca/P = 1.64. 'CaClAp' refers to calcium chlorapatite.

Table 2
Atomic ratios of Cl/M[a] in the near-surface region of the catalysts previously employed in the ethane oxidation in the presence of TCM at 773 K[b]

	CaHAp				SrHAp			
	M = Ca				M = Sr			
M/P[a]	1.64	1.60	1.55	1.51	1.73	1.70	1.67	1.61
Cl/M[a]	0.11 (0.11)	0.14 (0.14)	0.04 (0.02)	0.14 (0.08)	0.20 (0.20)	0.25 (0.25)	0.19 (0.17)	0.11 (0.07)

[a] M = Ca or Sr.
[b] CaHAp and SrHAp were previously employed in obtaining the results shown in Fig. 1B and Fig. 3B, respectively, but after 6 h on-stream. Values in parentheses show those after argon-ion etching for 1 min.

In contrast with the observations on CaHAp the conversion of ethane on SrHAp, in the absence of TCM, decreased while the selectivities remained relatively unchanged with increasing Sr/P (Fig. 3A). With SrHAp the conversions were somewhat higher than those found with CaHAp while the selectivities to CO with the former were smaller than those observed with the latter catalyst. Since, as reported earlier, the oxidation of methane on SrHAp and CaHAp without TCM produces high selectivities to CO and CO_x, respectively [18–22,24,25], the oxidation process, particularly on SrHAp, appears to be significantly dependent on the reactant hydrocarbon. Upon addition of TCM into the feedstream on SrHAp of Sr/P = 1.67, 1.70 and 1.73, the conversion of C_2H_6 and the selectivity to CO_2 decreased while the selectivities to C_2H_4 and CO increased with time-on-stream (Fig. 3B). However, the catalytic activities on $SrHAp_{1.61}$ with TCM present were essentially independent of time-on-stream. The XRD pattern of $SrHAp_{1.61}$ previously employed in ethane oxidation with TCM showed that the predominant phase was strontium hydroxyapatite (JCPDS 33-1348) and a small amount of strontium chlorapatite (JCPDS 16-0666) and phosphate (JCPDS 24-1008) formed during the oxidation (Fig. 4A). In contrast, the remaining three catalysts converted completely to the corresponding chlorapatite (Fig. 4B–D). Therefore, the time-on-stream insensitivity of the activities on $SrHAp_{1.61}$ in the presence of TCM appears to be related to the incomplete conversion of SrHAp to the corresponding chlorapatite. However, the effects of the introduction of TCM and the time-on-stream on SrHAp of Sr/P = 1.67, 1.70 and 1.73 were quite different from those observed with the 1.61 catalyst (Fig. 3B) although the XRD patterns of the former catalysts after the oxidation with TCM were essentially identical (Fig. 4B–D). XPS analyses of the latter three catalysts suggest that the chlorination of SrHAp is strongly dependent on the stoichiometry of SrHAp (Table 2), resulting in

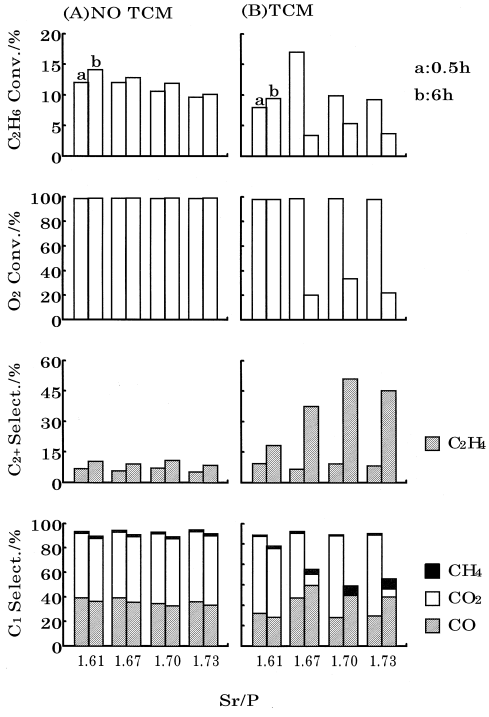

Fig. 3. Ethane oxidation on SrHAp in the absence (A) and presence (B) of TCM at 773 K. Conditions: same as those in Fig. 1.

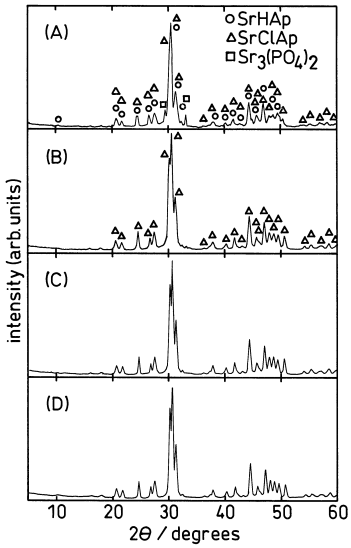

Fig. 4. XRD patterns of SrHAp previously employed in obtaining the results shown in Fig. 3B but after 6 h on-stream. (A) Sr/P = 1.61, (B) Sr/P = 1.67, (C) Sr/P = 1.70, (D) Sr/P = 1.73 'SrClAp' refers to strontium chlorapatite.

dissimilar TCM effects (Fig. 3B). As expected from the XRD data (Fig. 4A) the concentration of surface chlorinated species on $SrHAp_{1.61}$ was significantly smaller than observed with any of the remaining stoichiometries. Analogous with the results for CaHAp, this chlorinated species appears to be strontium chlorapatite. The differences in the conversion and the selectivities on $SrHAp_{1.67}$ and $SrHAp_{1.70}$, particularly at the higher time-on-stream in the presence of TCM should be noted although the quantities of chlorinated species are essentially identical on both SrHAp. The effect of the introduction of TCM into the ethane oxidation feedstream is evidently dependent upon the stoichiometry of SrHAp as well as the concentration of O_2 and TCM.

In view of the dependence of the effects of TCM on the reaction conditions the remainder of this report focuses on the effects of the concentration of O_2 and TCM with the stoichiometric hydroxyapatites $CaHAp_{1.60}$ and $SrHAp_{1.61}$.

Although the partial pressure of oxygen in the feedstream was increased up to 20 kPa, the oxidation of ethane without TCM on both $CaHAp_{1.60}$ and $SrHAp_{1.61}$ could not be released from the oxygen limiting conditions (Fig. 5A and Fig. 6A, respectively). The selectivities to CO and CO_2 increased and decreased, respectively, with increasing partial pressure of O_2 while the selectivity to C_2H_4 was little influenced by the partial pressure on both $CaHAp_{1.60}$ and $SrHAp_{1.61}$. Upon addition of TCM and with increasing time-on-stream, the conversion of C_2H_6 and the selectivity to CO_2 decreased markedly concomitant with increases in the selectivity to C_2H_4 at $P(O_2) = 6.7$ and 20.0 kPa on $CaHAp_{1.60}$ and 13.3 and 20.0 kPa on $SrHAp_{1.61}$ while the conversion of C_2H_6 decreased mildly and the selectivity was little influenced at $P(O_2) = 13.3$ kPa on $CaHAp_{1.60}$ and 6.7 kPa on $SrHAp_{1.61}$ (Fig. 5B and Fig. 6B, respectively). Even when the partial pressure of TCM was increased, the effects of the introduction of TCM on the oxidation process strongly depended on the partial pressure with either

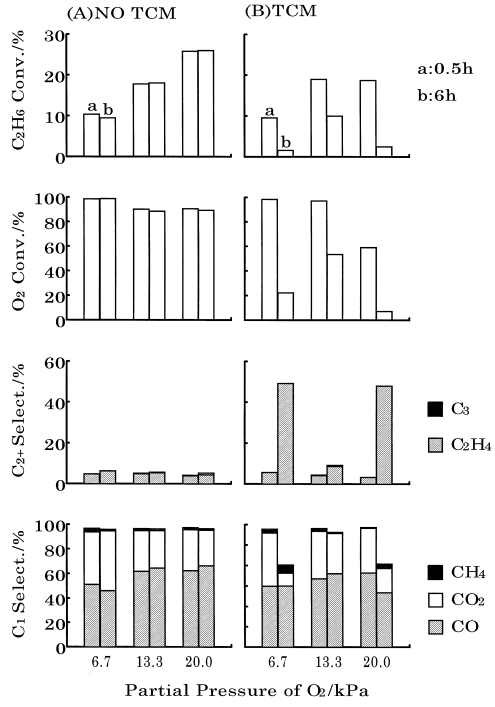

Fig. 5. Effects of the partial pressure of O_2 on ethane oxidation in the absence (A) and presence (B) of TCM on $CaHAp_{1.60}$ at 773 K. Conditions: same as those in Fig. 1 except $P(O_2)$.

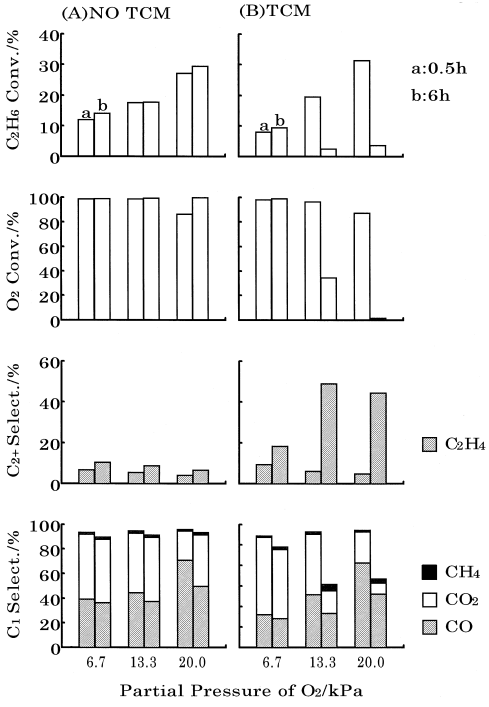

Fig. 6. Effects of the partial pressure of O_2 on ethane oxidation in the absence (A) and presence (B) of TCM on $SrHAp_{1.61}$ at 773 K. Conditions: same as those in Fig. 1 except $P(O_2)$.

catalyst (Fig. 7). On $CaHAp_{1.60}$, the change in the conversion of C_2H_6 with time-on-stream diminished with increasing P(TCM) up to 0.34 kP and increased at P(TCM) = 0.68 kPa, where the decrease of CO_2 selectivity and the substantial enhancement of the selectivity to C_2H_4 as obtained at P(TCM) = 0.17 and 0.34 kPa were not observed (Fig. 7A). In contrast, the decrease of the conversion of C_2H_6 and the selectivity to CO_2 together with the increase of the selectivity to C_2H_4 with increasing time-on-stream were observed only at P(TCM) = 0.34 kPa on $SrHAp_{1.61}$. At P(TCM) = 0.17 and 0.68 kPa, activities changed relatively little with increasing time-on-stream although the conversion of C_2H_6 at both partial pressures of TCM was smaller than that in the absence of TCM (cf. Fig. 3B and Fig. 7B).

As shown in Fig. 8, the XRD patterns of $CaHAp_{1.60}$ previously employed in the oxidation of ethane depended on the partial pressure of O_2 and TCM in the feedstream. Although one phase of calcium chlorapatite was detected in $CaHAp_{1.60}$ previously employed at our standard conditions of $P(O_2) = 6.7$ and P(TCM) = 0.17 kPa (Fig. 2C), with the increase of $P(O_2)$ to 13.3 kPa, the principal phase remained as CaHAp while small quantities of chlorapatite and calcium phosphate were also observed (Fig. 8A). Since, under the latter conditions, a small quantity of the surface chlorinated species was detected (Table 3), the relatively minor effects of the introduction of TCM on the oxidation of ethane (Fig. 5B, P(TCM) = 13.3 kPa) may be reasonable. After a further increase of the partial pressure to 20.0 kPa, the hydroxyapatite had completely disappeared and a mixture of the chlorapatite and phosphate was detected (Fig. 8B), whose pattern was essentially identical to that of $CaHAp_{1.60}$ previously used at $P(O_2)$ = 6.7 and P(TCM) = 0.34 kPa (Fig. 8C). On

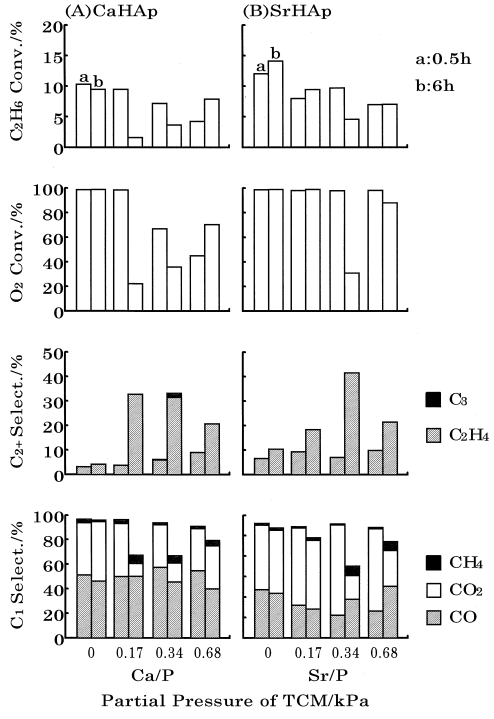

Fig. 7. Effects of the partial pressure of TCM on ethane oxidation on $CaHAp_{1.60}$ (A) and $SrHAp_{1.61}$ (B) at 773 K. Conditions: same as those in Fig. 1 except P(TCM).

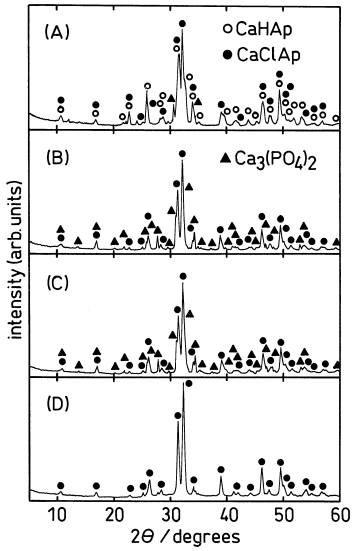

Fig. 8. XRD patterns of $CaHAp_{1.60}$ previously employed in obtaining the results shown in Fig. 5B and Fig. 7A but after 6 h on-stream. (A) $P(O_2) = 13.3$ kPa, P(TCM) = 0.17 kPa in Fig. 5B. (B) $P(O_2) = 20.0$ kPa, P(TCM) = 0.17 kPa in Fig. 5B. (C) $P(O_2) = 6.7$ kPa, P(TCM) = 0.34 kPa in Fig. 7A. (D) $P(O_2) = 6.7$ kPa, P(TCM) = 0.68 kPa in Fig. 7A.

$CaHAp_{1.60}$ previously employed under those conditions, relatively large quantities of chlorinated species were detected (Table 3), leading to the similar effects of the introduction of TCM on the oxidation (Fig. 5B, $P(O_2) = 20.0$ kPa and Fig. 6, P(TCM) = 0.34 kPa). Only the chlorapatite was again detected in the catalyst previously employed at P(TCM) = 0.68 kPa (Fig. 8D) with an XRD pattern essentially identical to that of the catalysts previously employed under the standard conditions. However, the activities with increasing time-on-stream were quite different (Fig. 7A, P(TCM) = 0.68 kPa and Fig. 1B, respectively). More chlorinated species were formed on the surface of $CaHAp_{1.60}$ previously employed at P(TCM) = 0.68 kPa, than that used at the standard conditions, suggesting that other chlorinated species together with the chlorapatite may be present on the surface and contribute to the oxidation of ethane in the presence of TCM. Similar conclusions can be drawn from the corresponding data obtained with $SrHAp_{1.61}$, the XRD patterns for which previously employed at various partial pressures of O_2 and TCM were identical (Fig. 9) but the effects of TCM were quite different (Fig. 6B and Fig. 7B). Although differences in the quantities of chlorinated species formed on the surface of $SrHAp_{1.61}$ were not evident (Table 3),

Table 3
Atomic ratios of Cl/M[a] in the near-surface region of $CaHAp_{1.60}$ and $SrHAp_{1.61}$ previously employed in the ethane oxidation at various concentrations of O_2 and TCM at 773 K[b]

$P(O_2)$ /kPa		13.3	20.0	6.7	6.7
P(TCM) /kPa		0.17	0.17	0.34	0.68
Catalyst	Cl/M				
$CaHAp_{1.60}$	Cl/Ca	0.07	0.19	0.16	0.22
		(0.06)	(0.16)	(0.13)	(0.20)
$SrHAp_{1.61}$	Cl/Sr	0.19	0.21	0.18	0.25
		(0.15)	(0.17)	(0.19)	(0.19)

[a] M = Ca or Sr.
[b] $CaHAp_{1.60}$ and $SrHAp_{1.61}$ were previously employed in obtaining the results shown in Figs. 5–7 but after 6 h on-stream.
Values in parentheses show those after argon-ion etching for 1 min.

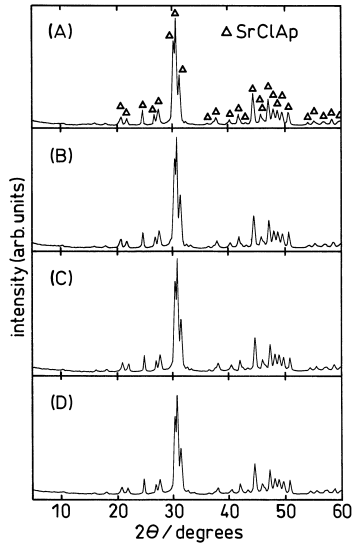

Fig. 9. XRD patterns of $SrHAp_{1.61}$ previously employed in obtaining the results shown in Fig. 6B and Fig. 7B but after 6 h on-stream. (A) $P(O_2) = 13.3$ kPa, P(TCM) = 0.17 kPa in Fig. 6B. (B) $P(O_2) = 20.0$ kPa, P(TCM) = 0.17 kPa in Fig. 6B. (C) $P(O_2) = 6.7$ kPa, P(TCM) = 0.34 kPa in Fig. 7B. (D) $P(O_2) = 6.7$ kPa, P(TCM) = 0.68 kPa in Fig. 7B.

other chlorinated species may contribute to the oxidation process.

Although the identification of the other chlorinated species formed on the surface of CaHAp and SrHAp is not clear in the present study, the corresponding chlorides, $CaCl_2$ and $SrCl_2$, are probably formed. In the hydroxyapatite system, the chlorides may be produced through deep chlorination of the hydroxyapatite to chloride through the chlorapatite [28], or by chlorination of the phosphate, converting from the hydroxyapatite [24], to the chloride [27]. It has been already reported that the selectivities to C_2H_4 on alkaline earth phosphate catalysts were dramatically enhanced by the introduction of TCM into the ethane oxidation feedstream and the formation of the corresponding chloride during the oxidation was suggested as a major contributor [27]. It should be pointed out that the chlorapatite which formed in the oxidation of ethane at high conversions [29] may be converted to the corresponding phosphate with an excess of H_2O at temperatures as low as 773 K.

4. Conclusions

(1) Non-selective formation of CO_x was observed on CaHAp and SrHAp in the oxidation of ethane without TCM although carbon monoxide is selectively formed in the oxidation of methane on SrHAp [24,25].

(2) The conversion of CaHAp and SrHAp to the corresponding chlorapatite resulted in the decrease of the conversion of ethane and the selectivity to CO_2 with increasing time-on-stream. These influences of the formation of the chlorapatite are identical to those observed in the oxidation of methane on both catalysts [20–24].

(3) The catalytic activities of the corresponding phosphate, which was detected by XRD in $CaHAp_{1.55}$ previously employed in ethane oxidation with TCM (Fig. 2B), may be similar to those of the corresponding chlorapatite converted from $CaHAp_{1.64}$ (Fig. 1B and Fig. 2D). However, both the chlorapatite and the chloride may form from the phosphate. The catalytic activities of CaHAp for the oxidation of methane in the absence of TCM are significantly higher than those on the corresponding phosphate [22].

(4) The mechanism through which the chlorinated species contribute to the oxidation of ethane in the presence of TCM is, as yet, unclear. While the evidence favours the participation of surface chlorine in the process with the chlorapatite as the principal surface chlorinated species the contribution of other forms of chlorine contained within the catalyst cannot be dismissed. Regardless of the mechanism, the selectivity to C_2H_4 is a beneficiary of the surface chlorine.

Acknowledgements

This work was partially funded by a ‘Grant for Natural Gas Research’ of The Japan Petroleum Institute to S.S., and the Natural Science and Engineering Research Council of Canada to J.B.M., to which our thanks are due.

References

[1] V. Soenen, J.M. Herrmann, J.C. Volta, J. Catal. 159 (1996) 410.
[2] T. Masuda, J. Natl. Chem. Lab. Ind. 87 (1992) 147.
[3] M. Tamura, M. Ishino, T. Deguchi, S. Nakamura, J. Organomet. Chem. 312 (1986) C75.
[4] Y. Kiso, K. Saeki, T. Hayashi, M. Tanaka, Y. Matsunaga, M. Ishino, M. Tamura, T. Deguchi, S. Nakamura, J. Organomet. Chem. 335 (1987) C27.
[5] S. Nakamura, Chemtech. (1990) 556.
[6] H. Arakawa, T. Hanaoka, K. Takeuchi, T. Matsuzaki, Y. Sugi, Chem. Lett. (1984) 1607.
[7] H. Hamada, R. Funaki, Y. Kuwahara, T. Kintaichi, K. Wakabayashi, T. Ito, Appl. Catal. 30 (1987) 177.
[8] T. Matsuzaki, K. Takeuchi, T. Hanaoka, H. Arakawa, Y. Sugi, Catal. Today 28 (1996) 251.
[9] T. Navajo, K. Sano, S. Matsuhira, H. Arakawa, J. Chem. Soc., Chem. Commun. (1987) 647.
[10] H. Arakawa, Y. Kiyozumi, K. Suzuki, K. Takeuchi, T. Matsuzaki, Y. Sugi, T. Fukushima, S. Matsushita, Chem. Lett. (1986) 1341.
[11] J.A.S. Bett, L.G. Christner, W.K. Hall, J. Catal. 13 (1969) 332.
[12] C.L. Kibby, W.K. Hall, J. Catal. 29 (1973) 144.

[13] C.L. Kibby, W.K. Hall, J. Catal. 31 (1973) 65.
[14] H. Monma, J. Catal. 75 (1982) 200.
[15] Y. Imizu, M. Kadoya, H. Abe, Chem. Lett. (1982) 415.
[16] Y. Izumi, S. Sato, K. Urabe, Chem. Lett. (1983) 1649.
[17] H. Monma, Skokubai 27 (1985) 237, in Japanese, Catalysts and Catalysis.
[18] Y. Matsumura, J.B. Moffat, Catal. Lett. 17 (1993) 197.
[19] Y. Matsumura, J.B. Moffat, J. Catal. 148 (1994) 323.
[20] S. Sugiyama, T. Minami, H. Hayashi, M. Tanaka, N. Shigemoto, J.B. Moffat, J. Chem. Soc., Faraday Trans. 92 (1996) 293.
[21] S. Sugiyama, T. Minami, T. Moriga, H. Hayashi, K. Koto, M. Tanaka, J.B. Moffat, J. Mater. Chem. 6 (1996) 459.
[22] S. Sugiyama, T. Minami, H. Hayashi, M. Tanaka, N. Shigemoto, J.B. Moffat, Energy Fuels 10 (1996) 828.
[23] Y. Matsumura, S. Sugiyama, H. Hayashi, N. Shigemoto, K. Saitoh, J.B. Moffat, J. Mol. Catal. 92 (1994) 81.
[24] S. Sugiyama, T. Minami, H. Hayashi, M. Tanaka, J.B. Moffat, J. Solid State Chem. 126 (1996) 242.
[25] S. Sugiyama, T. Minami, T. Higaki, H. Hayashi, J.B. Moffat, Ind. Eng. Chem. Res. 36 (1997) 328.
[26] J.B. Moffat, S. Sugiyama, H. Hayashi, Catal. Today 37 (1997) 15.
[27] S. Sugiyama, N. Kondo, K. Satomi, H. Hayashi, J.B. Moffat, J. Mol. Catal. A 95 (1995) 35.
[28] S. Sugiyama, H. Nishioka, T. Moriga, H. Hayashi, J.B. Moffat, Abstract of the 62nd National Meeting of the Society of Chemical Engineers, Japan, 3 (1997) 213.
[29] S. Sugiyama, K. Abe, T. Miyamoto, H. Hayashi, J.B. Moffat, J. Mol. Catal. A 130 (1998) 297.